HOKKAIDO UNIVERSITY

| | |
|---|---|
| Title | Rotaxane Formation of Multicyclic Polydimethylsiloxane in a Silicone Network: A Step toward Constructing "Macro-Rotaxanes" from High-Molecular-Weight Axle and Wheel Components |
| Author(s) | Ebe, Minami; Soga, Asuka; Fujiwara, Kaiyu; Ree, Brian J.; Marubayashi, Hironori; Hagita, Katsumi; Imasaki, Atsushi; Baba, Miru; Yamamoto, Takuya; Tajima, Kenji; Deguchi, Tetsuo; Jinnai, Hiroshi; Isono, Takuya; Satoh, Toshifumi |
| Citation | Angewandte chemie-international edition, 62(35), e202304493<br>https://doi.org/10.1002/anie.202304493 |
| Issue Date | 2023-08-28 |
| Doc URL | http://hdl.handle.net/2115/92776 |
| Rights | This is the peer reviewed version of the following article: Ebe, M., Soga, A., Fujiwara, K., Ree, B. J., Marubayashi, H., Hagita, K., Imasaki, A., Baba, M., Yamamoto, T., Tajima, K., Deguchi, T., Jinnai, H., Isono, T., Satoh, T., Angew. Chem. Int. Ed. 2023, 62, e202304493, which has been published in final form at https://doi.org/10.1002/anie.202304493. This article may be used for non-commercial purposes in accordance with Wiley Terms and Conditions for Use of Self-Archived Versions. This article may not be enhanced, enriched or otherwise transformed into a derivative work, without express permission from Wiley or by statutory rights under applicable legislation. Copyright notices must not be removed, obscured or modified. The article must be linked to Wiley ' s version of record on Wiley Online Library and any embedding, framing or otherwise making available the article or pages thereof by third parties from platforms, services and websites other than Wiley Online Library must be prohibited. |
| Type | article (author version) |
| File Information | Angew. Chem.-Int. Edit.62(35)e202304493.pdf |

Instructions for use

Hokkaido University Collection of Scholarly and Academic Papers : HUSCAP

RESEARCH ARTICLE

# *Rotaxane Formation of Multicyclic Polydimethylsiloxane in a Silicone Network: A Step toward Constructing "Macro-Rotaxanes" from High-Molecular-Weight Axle and Wheel Components*

Minami Ebe [b], Asuka Soga [b], Kaiyu Fujiwara [b], Brian J. Ree [a], Hironori Marubayashi [c], Katsumi Hagita [d], Atsushi Imasaki [c], Miru Baba [a], Takuya Yamamoto [a], Kenji Tajima [a], Tetsuo Deguchi [e], Hiroshi Jinnai [c], Takuya Isono [a]*, and Toshifumi Satoh [a]*

[a] Brian J. Ree, Miru Baba, Takuya Yamamoto, Kenji Tajima, Takuya Isono, and Toshifumi Satoh
Division of Applied Chemistry, Faculty of Engineering
Hokkaido University
Sapporo 060-8628, Japan
E-mail: isono.t@eng.hokudai.ac.jp, satoh@eng.hokudai.ac.jp
[b] Minami Ebe, Asuka Soga, and Kaiyu Fujiwara
Graduate School of Chemical Sciences and Engineering
Hokkaido University
Sapporo 060-8628, Japan
[c] Hironori Marubayashi, Atsushi Imasaki, and Hiroshi Jinnai
Institute of Multidisciplinary Research for Advanced Materials
Tohoku University
Sendai 980-8577, Japan
[d] Katsumi Hagita
Department of Applied Physics
National Defense Academy
Yokosuka 239-8686, Japan
[e] Tetsuo Deguchi
Department of Physics, Faculty of Core Research
Ochanomizu University
Tokyo 112-8610, Japan

Supporting information for this article is given via a link at the end of the document.

**Abstract:** Rotaxanes consisting of a high-molecular-weight axle and wheel components (macro-rotaxanes) have high structural freedom, and are attractive for soft-material applications. However, their synthesis remains underexplored. Here, we investigated macro-rotaxane formation via topological trapping of multicyclic polydimethylsiloxanes (*mc*-PDMSs) in silicone networks. *mc*-PDMS with different numbers of cyclic units and ring sizes were synthesized by cyclopolymerization of a *α,ω*-norbornenyl-functionalized PDMS. Silicone networks were prepared in the presence of 10–60 wt% *mc*-PDMS, and the trapping efficiency of *mc*-PDMS was determined. Contrary to monocyclic PDMS, *mc*-PDMSs with more cyclic units and larger ring sizes can be quantitatively trapped in the network as macro-rotaxanes. The damping performance of a 60 wt% *mc*-PDMS-blended silicone network was evaluated, revealing a higher tan *δ* than the bare PDMS network. Thus, macro-rotaxanes are promising as non-leaching additives for network polymers.

## Introduction

A rotaxane is a mechanically interlocked structure in which a linear molecule (axle component) penetrates a cyclic molecule (wheel component) (Figure 1(a)). A bulky stopper at the end of the axle component enables the two parts to connect without covalent bonding. Such supramolecular systems hold promise for many nanotechnological applications such as nanomachines,[1,2] molecular motors,[3] and vitrimers.[4] Although the main focus of such supramolecular systems has been on well-defined small molecules, the emergence of polyrotaxanes,[5,6] which use linear polymers as axles, has led to more practical applications, such as slide-ring materials (Figure 1(b,c)). Because polyrotaxanes accept multiple wheel components and each can shuttle freely along the linear polymer, they have been successfully applied as movable cross-links for toughening gels,[7,8] plastics,[9] and elastomers[10] through the effective release of stress concentration. However, a rotaxane system consisting of high-molecular-weight axle and wheel components, which can be termed a "macro-rotaxane", has not been considered; such a system is of considerable interest for soft-material applications because of its high degree of structural freedom.

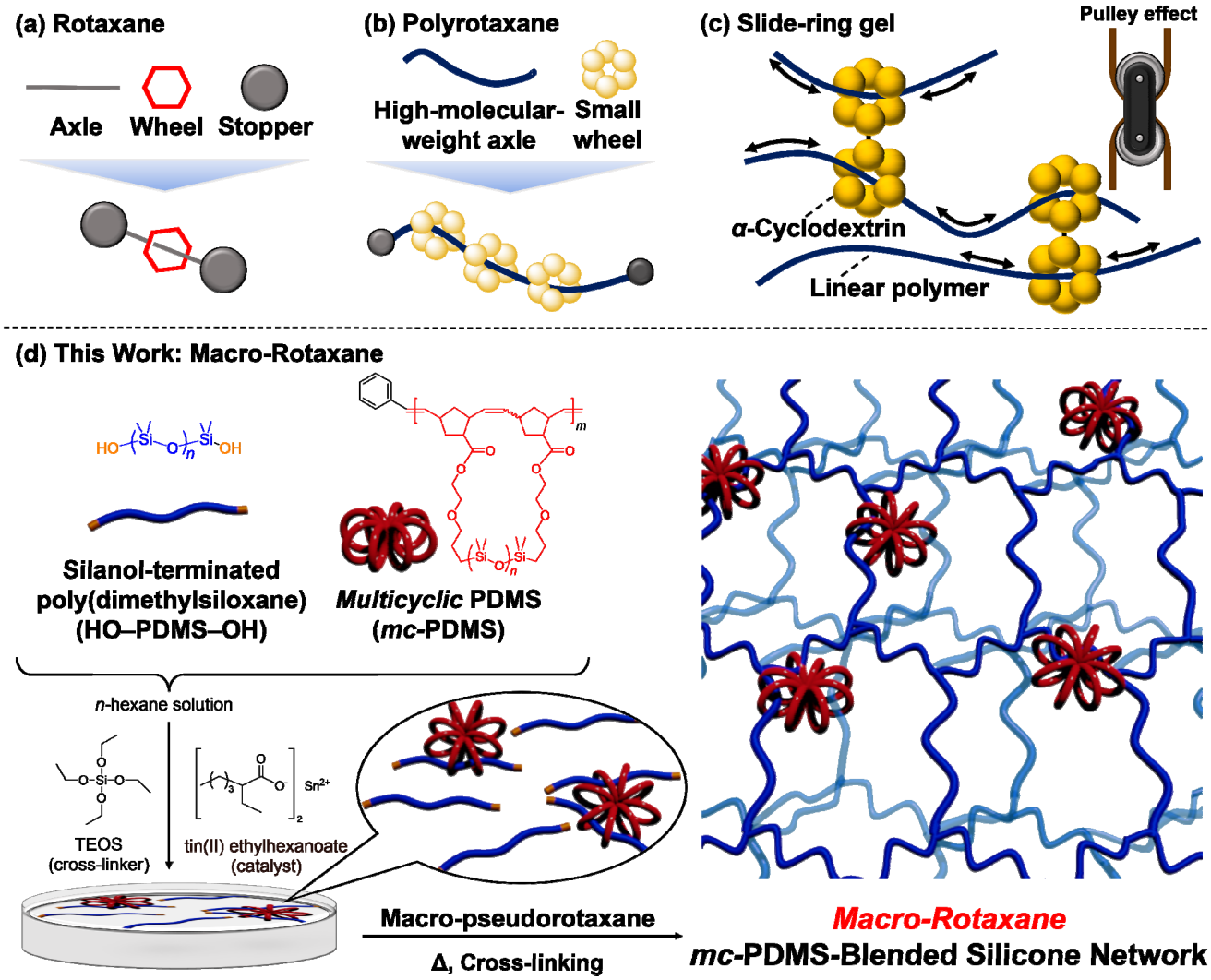


**Figure 1.** Schematic illustrations of various types of rotaxane structures. Rotaxanes with small axle and wheel components (a). Polyrotaxane with a high-molecular-weight axle and small wheel components (b) and its application as movable cross-links for slide-ring materials (c). This work: synthesis and structure of a macro-rotaxane consisting of high-molecular-weight axle and wheel components (d).

In theory, a mixture of linear and cyclic polymers should produce "macro-pseudorotaxanes". Several reported linear-cyclic polymer blend systems showed clues of macro-pseudorotaxane formation. For example, the addition of linear poly(ε-caprolactone) (PCL) to cyclic PCL lowered its crystallization and melting temperatures[11,12] and cyclic poly(ethylene glycol) (PEG) significantly reduced the crystallization temperature of linear PEG.[13] In addition, the crystallization of linear poly(L-lactide) (PLLA) was suppressed by the addition of a small amount of cyclic PLLA.[14] In amorphous linear-cyclic polymer blends, the viscoelasticity of cyclic polystyrene (PS) was significantly increased by the addition of a small amount of linear PS.[15–17] The viscoelasticity of linear PS was also increased by adding a small amount of cyclic PS, suggesting transient cross-link formation by the penetration of linear PS into cyclic PS,[18] the formation of this macro-pseudorotaxane is supported by molecular dynamics (MD) simulations.[19–22] A recent MD study demonstrated that linear-cyclic polymer blends have a negative Flory–Huggins interaction parameter, indicating that macro-pseudorotaxane formation occurs spontaneously.[23] The increase in conformational entropy of the cyclic chain upon threading is the main driving force of macro-pseudorotaxane formation. This contrasts with other rotaxane systems, where the formation is enthalpy-driven.

The end-capping of macro-pseudorotaxanes is essential for their material application. This is easily achieved by cross-linking the chain ends of the axle, as the cross-linking points act as stoppers to prevent de-threading of the wheels (Figure 1(d)). A few examples have been reported of trapping cyclic polymers in polymer networks by chemically cross-linking the linear chain ends in the presence of cyclic polymers.[24–31] This concept is referred to as topological trapping and was originally developed to verify the cyclic architecture of polymers. We revisited this concept to synthesize macro-rotaxanes for functional material applications. The first example of the preparation of polydimethylsiloxane (PDMS) networks in the presence of monocyclic PDMS was reported by Semlyen *et al.*[24,25] The effectiveness of topological trapping depended on the molecular weight of the cyclic polymers. For example, Semlyen, DeBolt, and

Clarson *et al.* reported trapping efficiencies of approximately 25% and 94% when the molecular weights of cyclic PDMS were 4,000 and 19,200, respectively.[24–27] The topological trapping of a cyclic polymer in chemically different polymer networks was also examined. Semlyen *et al.* reported the trapping of cyclic poly(11-undecalactone) in a PDMS network with an efficiency of up to 50%[28] and of cyclic PDMS in a poly(2,6-dimethyl-1,4-phenylene oxide) network with an efficiency of 36%.[29,30] A recent study by Waymouth *et al.* revealed that 36% of cyclic poly(2-isopropoxy-2-oxo-1,3,2-dioxaphospholane) was trapped in cross-linked 2-hydroxyethyl methacrylate hydrogels.[31] However, the practical material application of these macro-rotaxane systems has not been achieved because of their generally low trapping efficiencies. Moreover, the difficulty in preparing cyclic polymers has hindered their synthesis application. In particular, no experimental study has been reported on the impact of wheel component topology on macro-rotaxane formation and its properties.

In this study, we extended the concept of topological trapping to multicyclic polymers to develop macro-rotaxanes, a novel type of mechanically interlocked networks. Although previous topological trapping studies have only been performed on monocyclic polymers, our recent coarse-grained molecular dynamics (CGMD) simulations revealed that trapping probability in cross-linked networks increases with the number of cyclic units of the polymer.[32] Therefore, multicyclic polymers should lead to quantitative topological trapping. Multicyclic polymers can also function as movable cross-linking points. In fact, the first example of a slide-ring gel[7] utilized *α*-cyclodextrin dimers (i.e., a bicyclic wheel component) as the movable cross-linking point, similar to a molecular pulley (Figure 1(c)). Our CGMD simulation demonstrated that multicyclic polymers have multiple linear chain penetrations, even for small-sized rings.[33] More importantly, multicyclic polymers showed a higher ring-bridge formation probability than monocyclic polymers (Figure 2).[32] An increased ring-bridge probability is vital for bulk material applications because bridging rings can act as movable cross-links, changing the mechanical properties of the material.

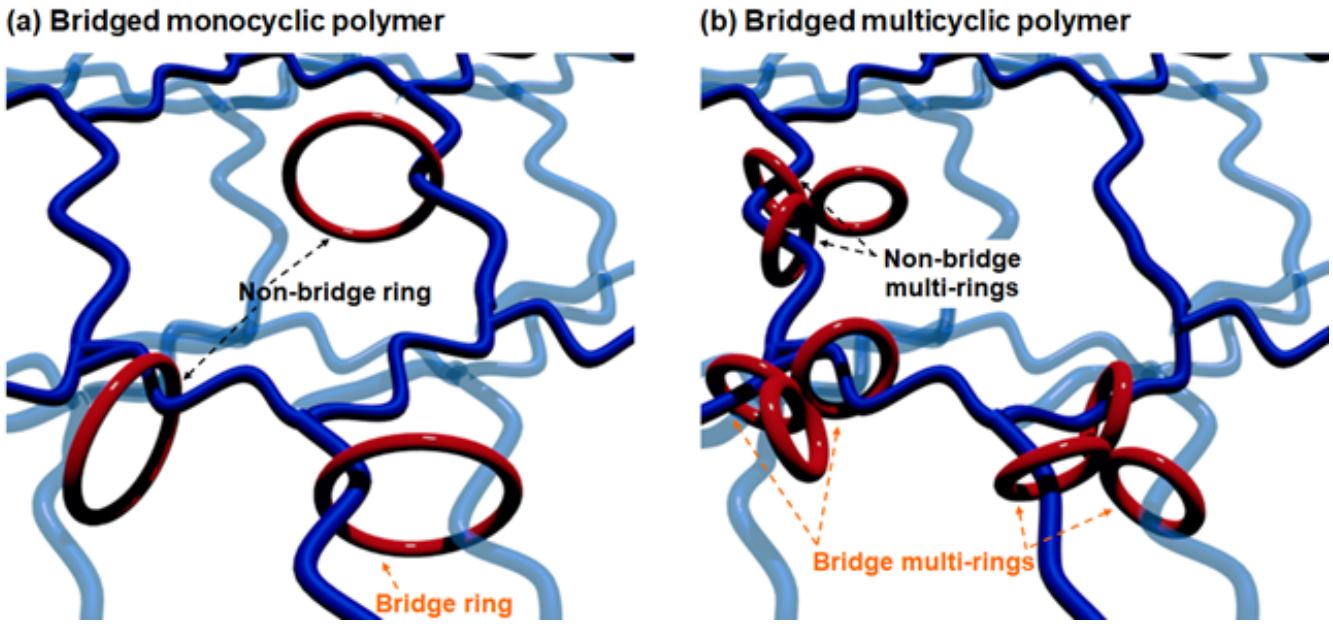


**Figure 2.** Schematic illustrations of the ring-bridge probability of macro-rotaxanes consisting of (a) monocyclic polymers and (b) multicyclic polymers as high-molecular-weight wheel components. Multicyclic polymers should have a higher ring-bridge probability than monocyclic polymers in cross-linked networks. Ring-bridge probability represents the probability that multiple chains penetrate a monocyclic or multicyclic polymer molecule.

Herein, we report the topological trapping of multicyclic PDMS in silicone networks to experimentally determine the impact of cyclic polymer topology on trapping efficiency and investigate macro-rotaxane formation. Although multicyclic polymer synthesis is challenging, we recently established a highly efficient synthetic pathway for multicyclic polymers that does not require a complicated multistep process.[34,35] Cyclopolymerization of *α,ω*-norbornenyl-functionalized macromonomers produces the desired multicyclic polymer with a controlled number of cyclic units and ring sizes via ring-opening metathesis polymerization (ROMP) using a Grubbs 3$^{rd}$-generation catalyst (G3) (Scheme 1a). This pathway affords multicyclic polymers in high yields from commercially available telechelic polymers in two steps, which is simpler than the synthesis of monocyclic polymers. Using cyclopolymerization, we successfully synthesized a series of multicyclic PDMSs (*mc*-PDMSs) with different numbers of cyclic units and ring sizes. Silicone networks were prepared in the presence of *mc*-PDMS and monocyclic PDMS to trap PDMS in the form of a rotaxane. A systematic evaluation of the trapping efficiency revealed that *mc*-PDMS was quantitatively trapped under specific conditions up to approximately 50 wt%, demonstrating the advantage of using multicyclic polymers for macro-rotaxane construction. Based on these promising results, we demonstrated the potential application of this multicyclic polymer-blended network as a damping material.

## Results and Discussion

First, we synthesized monocyclic PDMS (*1c*-PDMS), reference materials for the relevant multicyclic polymers, by preparing *α*,*ω*-divinyl end-functionalized PDMS and performing the subsequent ring-closing metathesis (RCM) reaction (Scheme 1b). Commercially available *α*,*ω*-carbinol-functionalized PDMS (HOR–PDMS$_{4k}$–ROH; number-average molecular weight ($M_n$) estimated by $^1$H NMR ($M_{n,NMR}$) = 4,200, $M_n$ estimated by size-exclusion chromatography (SEC) using polystyrene (PS) standards ($M_{n,SEC}$) = 4,600, and dispersity ($Đ_{SEC}$) = 1.75), was treated with 4-pentenoic acid in the presence of 1-(3-dimethylaminopropyl)-3-ethylcarbodiimide hydrochloride (EDC·HCl) as condensing agent and 4-dimethylaminopyridine (DMAP) as catalyst to produce VN–PDMS$_{4k}$–VN ($M_{n,NMR}$ = 4,300; $M_{n,SEC}$ = 4,300; $Đ_{SEC}$ = 1.75). Following the standard RCM protocol for the synthesis of macrocyclic polymers, VN–PDMS$_{4k}$–VN was successfully converted to the desired *1c*-PDMS$_{4k}$. This RCM reaction was performed using a Hoveyda-Grubbs 2$^{nd}$ generation catalyst (HG2), in $CH_2Cl_2$ at reflux temperature; VN–PDMS$_{4k}$–VN was highly diluted (0.10 mmol L$^{-1}$) to avoid intermolecular reactions. The $^1$H NMR spectrum of the product showed the disappearance of the signals at 5.88–5.76 and 5.10–4.97 ppm (protons *b* and *a*) corresponding to the terminal vinyl group of VN–PDMS$_{4k}$–VN, indicating that the RCM reaction was near-quantitative (Figure 3(a)).

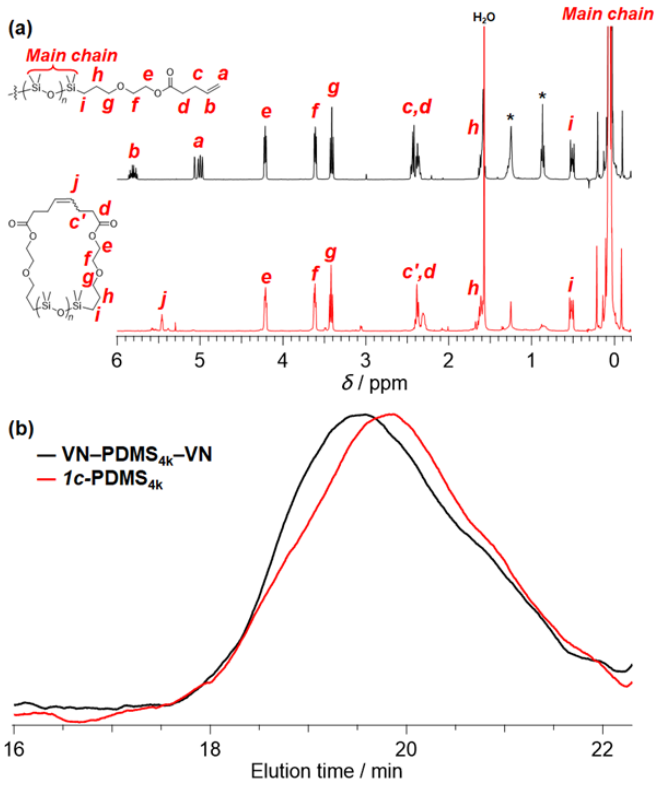


**Figure 3.** (a) $^1$H NMR (400 MHz, $CDCl_3$) spectra of VN–PDMS$_{4k}$–VN (black) and *1c*-PDMS$_{4k}$ (red). The asterisks represent residual *n*-hexane. (b) SEC traces of VN–PDMS$_{4k}$–VN (black) and *1c*-PDMS$_{4k}$ (red) (RI detection; eluent: THF).

The appearance of signals corresponding to the internal olefin formed in the cyclization (5.64–5.38 ppm; proton *j*) was also observed. SEC analysis of the obtained product revealed a $M_{n,SEC}$ of 3,700 and a monomodal elution peak with a $Đ_{SEC}$ of 1.84 (Figure 3(b)), suggesting that oligomerization via intermolecular reactions was suppressed. Importantly, the SEC peak-top molecular weights ($M_p$ = 5,300 against the linear PS standard) of the RCM product were smaller than those of VN–PDMS$_{4k}$–VN ($M_p$ = 6,900), supporting the decrease in the hydrodynamic radius due to cyclization. The compaction parameter ⟨G⟩, defined as the ratio $M_{p,cyclic}/M_{p,macromonomer}$, was calculated as 0.77, which is close to the value reported for monocyclic polymers.[36] These results confirmed the successful synthesis of *1c*-PDMS$_{4k}$. *1c*-PDMSs with different molecular weights (*1c*-PDMS$_{14k}$, *1c*-PDMS$_{28k}$, and *1c*-PDMS$_{37k}$) were also obtained using a similar protocol starting from *α*,*ω*-hydrosilane-functionalized PDMS.

The cyclopolymerization of *α*,*ω*-dinorbornenyl end-functionalized macromonomers is best option for the systematic synthesis of multicyclic PDMS (*mc*-PDMS) (Scheme 1b). *mc*-PDMS with different numbers of cyclic units and ring sizes are required to investigate the correlation between polymer topology and rotaxane-forming ability. Thus, a PDMS macromonomer, *α*,*ω*-dinorbornenyl end-functionalized PDMS (NB–PDMS$_{4k}$–NB; $M_{n,NMR}$ = 4,300), was prepared from HOR–PDMS$_{4k}$–ROH by its condensation with *exo*-5-norbornenecarboxylic acid (*exo*-NB–COOH) in the presence of EDC·HCl and DMAP in $CH_2Cl_2$. The $^1$H NMR spectrum of the product exhibited new signals at 6.16–6.07 and 3.07–2.89 ppm assignable to the norbornenyl group. Comparison of the signal intensities corresponding to the methylene groups adjacent to the main chain (0.58–0.45 ppm) and norbornenyl group (6.16–6.07 ppm) further confirmed the quantitative addition of the norbornenyl group at both chain ends. Notably, the protons of the methylene group adjacent to the terminal hydroxyl group (3.77–3.69 ppm) suffered an upfield shift to (4.27–4.18 ppm) upon condensation, confirming the near-quantitative conversion (Figure S1). SEC measurements of the product showed unimodal elution peaks, with estimated $M_{n,SEC}$ and $Đ_{SEC}$ values of 4,000 and 1.69, respectively. The NB–PDMS$_{4k}$–NB macromonomer was subjected to ROMP-based cyclopolymerization under highly dilute conditions to produce *mc*-PDMS. The controlled/living polymerization nature of G3-mediated ROMP allows the theoretical determination of the number of cyclic units from the initial [macromonomer]$_0$/[G3]$_0$ ratio. To synthesize *mc*-PDMS$_{4k}$ consisting of approximately three rings, the cyclopolymerization of NB–PDMS$_{4k}$–NB was performed in a highly diluted solution ([NB–PDMS$_{4k}$–NB]$_0$ = 0.10 mmol L$^{-1}$) with an initial [NB–PDMS$_{4k}$–NB]$_0$/[G3]$_0$ ratio of 3/1, in $CH_2Cl_2$ and under an Ar atmosphere. The high dilution is essential for intramolecular cyclization to prevail over intermolecular propagation, affording a cyclopolymerization without significant side reactions, such as gelation. The cyclopolymerization successfully proceeded without gelation, affording a soluble product in 86.2% yield after work-up to remove the catalyst. The $^1$H NMR spectrum of the product revealed quantitative monomer

conversion by the complete disappearance of the signals corresponding to the norbornenyl groups (6.16–6.07 ppm; protons *a* and *b*) (Figure 4(a)). In addition, broad signals derived from the oligo(norbornene) backbone (5.50–5.10, 3.18–1.86 ppm) were observed, confirming the

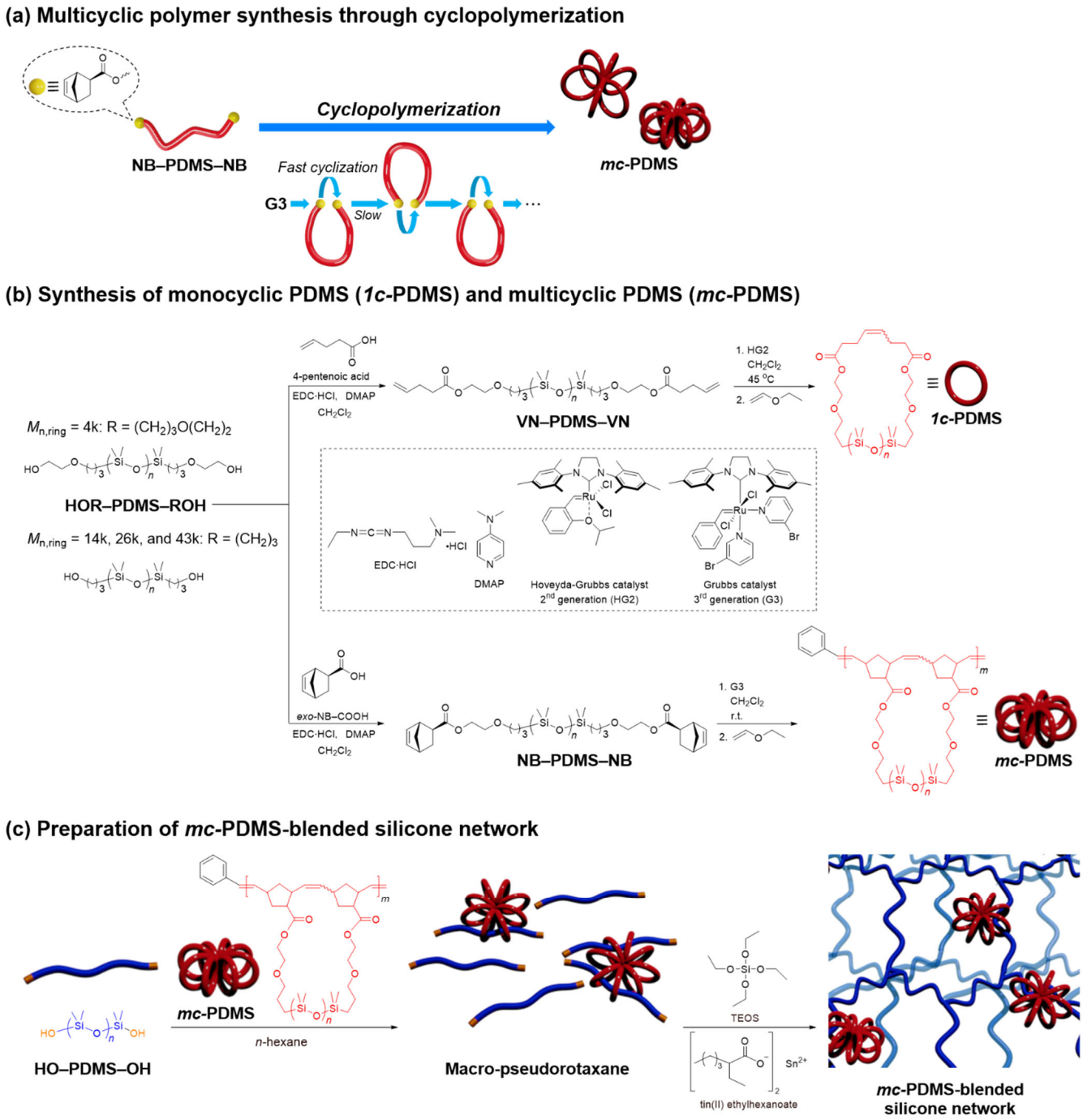


**Scheme 1.** (a) Schematic illustrations of cyclopolymerization (b) Synthetic routes for monocyclic PDMS (*1c*-PDMS) and multicyclic PDMS (*mc*-PDMS) (c) Preparation of a cyclic PDMS-blended silicone network

successful cyclopolymerization via ROMP. SEC measurements of the product revealed the complete consumption of the macromonomer, and the clear shift in the elution peak toward a higher molecular weight for the macromonomer further supported the cyclopolymerization mechanism (Figure 4(b)). Because conventional SEC does not provide meaningful molecular weight

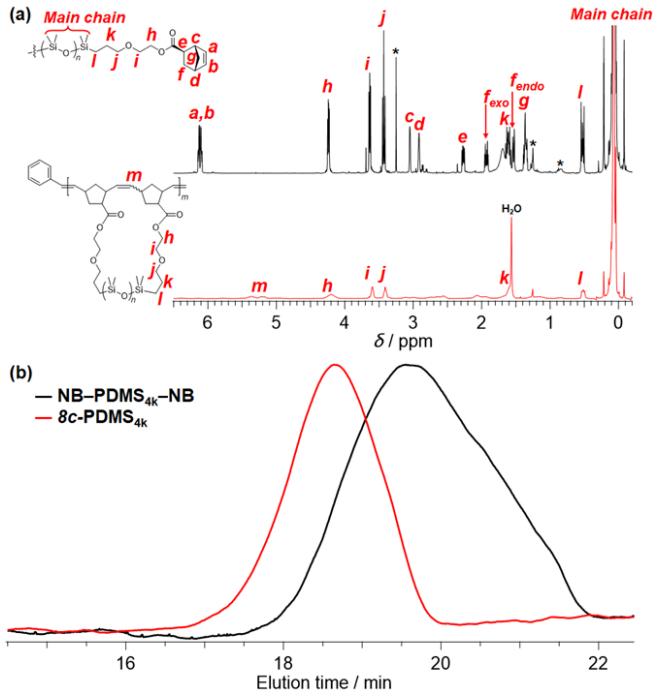


**Figure 4.** (a) $^1$H NMR (400 MHz, $CDCl_3$) spectra of NB–$PDMS_{4k}$–NB (black) and *8c*-$PDMS_{4k}$ (red). The asterisks represent residual solvents and impurities. (b) SEC traces of NB–$PDMS_{4k}$–NB (black) and *8c*-$PDMS_{4k}$ (red) (RI detection; eluent: THF).

information for our product owing to its nonlinear architecture, we used a triple-detection SEC equipped with multi-angle light scattering, viscosity, and refractive index detectors (SEC-MALS-Visco) to determine the absolute molecular weight ($M_{n,MALS}$). SEC-MALS-Visco analysis of the product determined $M_{n,MALS}$, and $Đ_{MALS}$ values of 34,400 and 1.25, respectively. *mc*-PDMS had eight cyclic units, calculated by dividing the $M_{n,MALS}$ of *mc*-PDMS by the $M_{n,NNR}$ of NB–$PDMS_{4k}$–NB. Based on the number of cyclic units and ring sizes, the obtained *mc*-PDMS was denoted as *8c*-$PDMS_{4k}$. Next, we performed the cyclopolymerization of NB–$PDMS_{4k}$–NB with varying initial macromonomer/initiator ratios to produce *mc*-PDMS with different numbers of cyclic units. Using the established reaction conditions while changing $[NB–PDMS–NB]_0/[G3]_0$ ratios to 4/1, 8/1, and 10/1 (runs 4–6), *mc*-PDMS with approximately 9 ($M_{n,MALS}$ = 37,700 and $Đ_{MALS}$ = 1.48), 12 ($M_{n,MALS}$ = 51,100 and $Đ_{MALS}$ = 1.20), and 25 ($M_{n,MALS}$ = 108,000 and $Đ_{MALS}$ = 1.56) cyclic units were successfully obtained in good yields (54–94%). Note here that the $Đ$ value of *mc*-PDMSs synthesized from the macromonomers is different. This can be explained by the dispersity arising from the number of cyclic units. Since the cyclic unit formation is based on the polymerization process, the obtained *mc*-PDMSs show dispersity due to the number of the cyclic units, which results in the variation of $Đ$ even from the same macromonomer. *mc*-PDMS with larger ring sizes (14k, 26k, and 43k) and varying numbers of cyclic units (4 or 11, 6 or 10, and 5, respectively) were synthesized by the cyclopolymerization of macromonomers of larger molecular weights (NB–$PDMS_{14k}$–NB, NB–$PDMS_{26k}$–NB, and NB–$PDMS_{43k}$–NB) (Table 1).

This cyclopolymerization approach is highly useful in controlling ring size and the number of cyclic units, enabling scalable synthesis. Most previous attempts at synthesizing multicyclic polymers have been small-scale (tens to hundreds of milligrams) because of complicated and multistep synthesis protocols. Taking advantage of our straightforward approach (only two steps from commercially available reagents), multicyclic PDMS with the desired ring size and number of cyclic units can now be easily accessed. In fact, the cyclopolymerization of 5.00 g of NB–$PDMS_{26k}$–NB produced 4.99 g of *6c*-$PDMS_{26k}$ (99.8% yield) in just a few hours.

A series of monocyclic and multicyclic PDMSs of varying ring sizes and numbers of cyclic units were used to construct cyclic PDMS-containing silicone networks. A tetrafunctional end-linked PDMS network was employed owing to its structural simplicity. These end-linked PDMS networks are typically synthesized using a platinum-mediated vinylsilane addition-based curing reaction.[37,38] However, this addition reaction is incompatible with our polymers because the cyclic and multicyclic PDMSs possess carbon–carbon double bonds. Thus, we selected the condensation reaction of silanol-terminated PDMS and tetraethyl orthosilicate (TEOS) to avoid unwanted covalent cross-linking between the network and monocyclic/multicyclic PDMS (Scheme 1c). Reproducibility of the synthesis is paramount for the fair comparison of the cyclic-containing and bare silicone networks. Therefore, we first established a protocol for preparing the silicone network, following a reported procedure with some modifications.[25,28,39–42] The silicone network was prepared by curing silanol-terminated PDMS (HO–$PDMS_{13k}$–OH; $M_{n,MALS}$ = 1.3 × $10^4$, $[HO–PDMS_{13k}–OH]_0$ = 0.13 g $mL^{-1}$) and TEOS with tin(II) 2-ethylhexanoate (0.5 wt%) in *n*-hexane. A slight excess of TEOS ($[TEOS]_0/[HO–PDMS_{13k}–OH]_0$ = 3/4) was added to ensure a complete reaction, thereby constructing a network with fewer structural defects. The curing was performed in an aluminum mold at 22–25 ºC under open air for 24 h to evaporate the solvent, followed by heating at 50 °C under high vacuum to complete the cross-linking reaction. Three silicone networks were prepared with varying curing times (1, 5, and 10 days) to optimize the curing time. Because the modulus of the network is proportional to cross-linking density, we employed a tensile test to evaluate the extent of the reaction. The Young's modulus was calculated from the initial slope of the stress–strain curves. Silicone networks cured for 5 and 10 days showed a Young's modulus of approximately 6.0 ± 0.58 kPa, which is higher than that of the network cured for a day (5.1 ± 0.14 MPa). Therefore, the cross-linking reaction reached saturation after 5 days of curing (Figure S2(a)). To check the reproducibility of the synthesis, we performed the same experiments (5 days of curing) at least three times. The stress–strain curves of samples from different batches overlapped well, confirming that the synthesized silicone networks had similar cross-link density (Figure S2(b)).

The spontaneous penetration of the linear chain into the cyclic chain to form the macro-pseudorotaxane has been confirmed by both experimental data and computational simulations.[11–23] The macro-pseudorotaxane is expected to be converted to rotaxane via *in situ* end-cross-linking. Having established a reproducible PDMS network synthesis, we applied it to the construction of a macro-rotaxane using monocyclic/multicyclic PDMS (10 wt%). All obtained silicone networks were visually transparent, suggesting that no macrophase separation occurred between the linear and *mc*-PDMS during cross-linking.

To the best of our knowledge, this is the first study to experimentally determine the systematic relationship between

**Table 1.** Molecular characterization of *1c*-PDMSs and different *mc*-PDMSs

| Run | Sample | Yield (%) | $M_{n,ring}$ [a] | $[G3]_0/[MM]_0$ | Cyclic units [b] | $M_{n,MALS}$ [c] | $Đ_{MALS}$ [c] | $M_{n,SEC}$ [d] | $Đ_{SEC}$ [d] |
|---|---|---|---|---|---|---|---|---|---|
| 1 [e] | HOR–PDMS$_{4k}$–ROH | - | 4,200 [f] | - | - | 6,400 | 1.66 | 4,600 | 1.75 |
| 2 | *1c*-PDMS$_{4k}$ | 92.0 | 4,300 | - | 1 | 10,900 | 1.36 | 3,700 | 1.84 |
| 3 | *8c*-PDMS$_{4k}$ | 86.2 | 4,300 | 1/3 | 8 | 34,400 | 1.25 | 14,400 | 1.28 |
| 4 | *9c*-PDMS$_{4k}$ | 61.1 | 4,300 | 1/4 | 9 | 37,700 | 1.48 | 20,600 | 1.18 |
| 5 | *12c*-PDMS$_{4k}$ | 93.8 | 4,300 | 1/8 | 12 | 51,100 | 1.20 | 15,900 | 1.29 |
| 6 | *25c*-PDMS$_{4k}$ | 53.7 | 4,300 | 1/10 | 25 | 108,000 | 1.56 | 30,600 | 1.15 |
| 7 [e] | HOR–PDMS$_{15k}$–ROH | - | 15,300 [f] | - | - | 10,900 | 1.21 | 13,100 | 1.06 |
| 8 | *1c*-PDMS$_{14k}$ | 72.0 | 14,000 | - | 1 | 30,400 | 2.20 | 12,800 | 1.09 |
| 9 | *4c*-PDMS$_{14k}$ | 88.9 | 14,200 | 1/3 | 4 | 55,800 | 1.28 | 36,500 | 1.37 |
| 10 | *11c*-PDMS$_{14k}$ | 91.6 | 14,200 | 1/10 | 11 | 155,800 | 1.22 | 89,000 | 1.36 |
| 11 [e] | HOR–PDMS$_{26k}$–ROH | - | 25,300 [f] | - | - | 27,700 | 1.42 | 25,900 | 1.36 |
| 12 | *1c*-PDMS$_{28k}$ | 65.6 | 27,900 | - | 1 | 16,600 | 1.19 | 21,700 | 1.31 |
| 13 | *6c*-PDMS$_{26k}$ | 99.8 | 25,500 | 1/3 | 6 | 145,300 | 2.37 | 87,800 | 1.98 |
| 14 | *10c*-PDMS$_{26k}$ | >99 | 25,500 | 1/10 | 10 | 245,000 | 2.53 | 107,000 | 2.83 |
| 15 [e] | HOR–PDMS$_{41k}$–ROH | - | *n.d.* [g] | - | - | 41,300 | 1.52 | 26,300 | 1.52 |
| 16 | *1c*-PDMS$_{37k}$ | 97.0 | *n.d.* [g] | - | 1 | 37,300 | 2.09 | 27,700 | 1.99 |
| 17 | *5c*-PDMS$_{43k}$ | 77.4 | *n.d.* [g] | 1/3 | 5 | 217,500 | 3.22 | 73,500 | 2.33 |

[a] Determined by $^1$H NMR spectroscopy (400 MHz, $CDCl_3$) of the macromonomers (MM: VN–PDMS–VN or NB–PDMS–NB). [b] The average number of cyclic units for multicyclic PDMSs was calculated as $M_{n,MALS}/M_{n,ring}$. [c] Determined by SEC-MALS, in $CHCl_3$. [d] Determined by SEC, in THF, using PS as the standard. [e] Runs 1, 7, 11, and 15 are precursors of cyclic PDMSs for runs 2–6, 8–10, 12–14, and 16–17, respectively. [f] $M_{n,NMR}$ of HOR–PDMS–ROH precursors. [g] Not determined by $^1$H NMR spectroscopy.

cyclic topology and ability to form macro-rotaxanes. To study rotaxane formation, we investigated the trapping efficiency by quantifying the amount of permanently trapped *mc*-PDMS in the network. Non-trapped *mc*-PDMS was eluted by soaking in toluene for five days. The trapping efficiency (%) was calculated as follows: (mass of *mc*-PDMS originally contained in the network – mass of non-trapped *mc*-PDMS) × 100 / mass of *mc*-PDMS originally contained in the network (see the Supporting Information for more details).

We focused on the trapping efficiency of a series of monocyclic and multicyclic PDMS with a fixed ring size of 4.3k ($M_{n,ring}$ = 4,300) (Table 2). The trapping efficiency of *1c*-PDMS$_{4k}$ was 27 ± 12% (*n* = 3), which matches that of a similar system reported by Semlyen *et al.*[24] Notably, 16% of linear PDMS of comparable molecular weight (*linear*-PDMS$_{4k}$) was trapped in the network after rigorous washing with boiling toluene using a Soxhlet extractor. These observations reveal insufficient rotaxane formation in the monocyclic PDMS with such a small ring, likely because the ring size (4.3k) is much smaller than the entanglement molecular weight ($M_e$) of PDMS (10,000–12,300).[43-47] An increase in the number of cyclic units significantly improved the trapping efficiency (79% for *9c*-PDMS$_{4k}$ and 92% for *25c*-PDMS$_{4k}$) for the same ring size because the penetration of a linear PDMS chain into only one of the rings results in permanent trapping in the network. Thus, a cyclic polymer chain can be quantitatively trapped in the network by optimizing the number of cyclic units, even for a ring size much smaller than the $M_e$. Notably, this trend matches the trapping probabilities obtained from our CGMD simulations of a blend of linear and multicyclic PDMS chains.[32]
We devised a fluorescent labeling approach to confirm the ring–number dependence of the topological trapping behavior. Silicone networks were prepared in the presence of pyrene-labeled *linear*-PDMS$_{4k}$, *1c*-PDMS$_{4k}$, *8c*-PDMS$_{4k}$, and *12c*-PDMS$_{4k}$ (see Scheme S1 in the Supporting Information for the pyrene-labeled PDMS synthesis), enabling the direct detection of trapped PDMS chains in the resulting networks from the fluorescence of pyrene groups. Silicone networks before and after soaking in toluene were observed under UV irradiation and the luminance was evaluated using a gel imager. A significant decrease in luminance was observed for *linear*-PDMS$_{4k}$ and *1c*-PDMS$_{4k}$ after soaking in toluene, but not for *8c*-PDMS$_{4k}$ and *12c*-PDMS$_{4k}$ (Figure 5). These results confirmed topological trapping through macro-rotaxane formation and an increasing trapping efficiency with increasing number of cyclic units.

Next, we investigated how the molecular weight of the network-forming linear HO–PDMS–OH (i.e., the axle component), which corresponds to the molecular weight between the cross-links ($M_c$) of the network,[41,42] affects macro-rotaxane formation. When using a large molecular weight HO–PDMS$_{80k}$–OH ($M_{n,MALS}$ = 8.0 × $10^4$), the trapping efficiency of *1c*-PDMS$_{4k}$ was 29%, within the range of that determined for the network obtained from HO–PDMS$_{13k}$–OH (27 ± 12%). This suggests that the molecular weight of the linear PDMS (axle) has a negligible impact on macro-rotaxane formation. Our previous CGMD simulations match this observation.[32] To confirm these results in more detail using *mc*-PDMS, we prepared PDMS networks synthesized from HO–PDMS$_{2k}$–OH ($M_{n,MALS}$ = 0.2 × $10^4$) and HO–PDMS$_{80k}$–OH ($M_{n,MALS}$ = 8.0 × $10^4$) in the presence of 10 wt% *16c*-PDMS$_{4k}$ ($M_{n,MALS}$ = 67,800, $Đ_{MALS}$ = 1.50), and compared them with the network obtained from HO–PDMS$_{13k}$–OH (Table 3). All silicone networks showed trapping efficiencies of 81–87% (87, 84, and 81% for HO–PDMS$_{2k}$–OH, HO–PDMS$_{13k}$–OH, and HO–PDMS$_{80k}$–OH, respectively), suggesting that the molecular weight of the linear PDMS is not the determining factor for macro-rotaxane formation. Thus, the most important factor is the ring size of the *mc*-PDMS.

**Table 2.** Trapping efficiencies determined for HO–PDMS$_{13k}$–OH silicone networks prepared in the presence of linear, monocyclic, and multicyclic PDMS [a]

| Run | Sample | Cyclic units [a] | Added PDMS (wt%) | % Trapped |
|---|---|---|---|---|
| 1 | *linear*-PDMS$_{4k}$ | - | 10 | 16 |
| 2 | *1c*-PDMS$_{4k}$ | 1 | | 27 ± 12 [b] |
| 3 | *9c*-PDMS$_{4k}$ | 9 | | 79 |
| 4 | *25c*-PDMS$_{4k}$ | 25 | | 92 |
| 5 | *linear*-PDMS$_{14k}$ | - | | 27 ± 4 [b] |
| 6 | *1c*-PDMS$_{14k}$ | 1 | | 40 |
| 7 | *4c*-PDMS$_{14k}$ | 4 | | 92 |
| 8 | *11c*-PDMS$_{14k}$ | 11 | | 100 |
| 9 | *1c*-PDMS$_{28k}$ | 1 | | 75 |
| 10 | | | 10 | 100 |
| 11 | *6c*-PDMS$_{26k}$ | 6 | 40 | 100 |
| 12 | | | 60 | 88 [c] |
| 13 | *10c*-PDMS$_{26k}$ | 10 | 10 | 100 |

[a] Calculated using [$M_{n,MALS}$ of *mc*-PDMS]/[$M_{n,NMR}$ of its macromonomer]. [b] Average value for at least two experiments. [c] The lowest value guaranteed based on the mass of the soluble fraction.

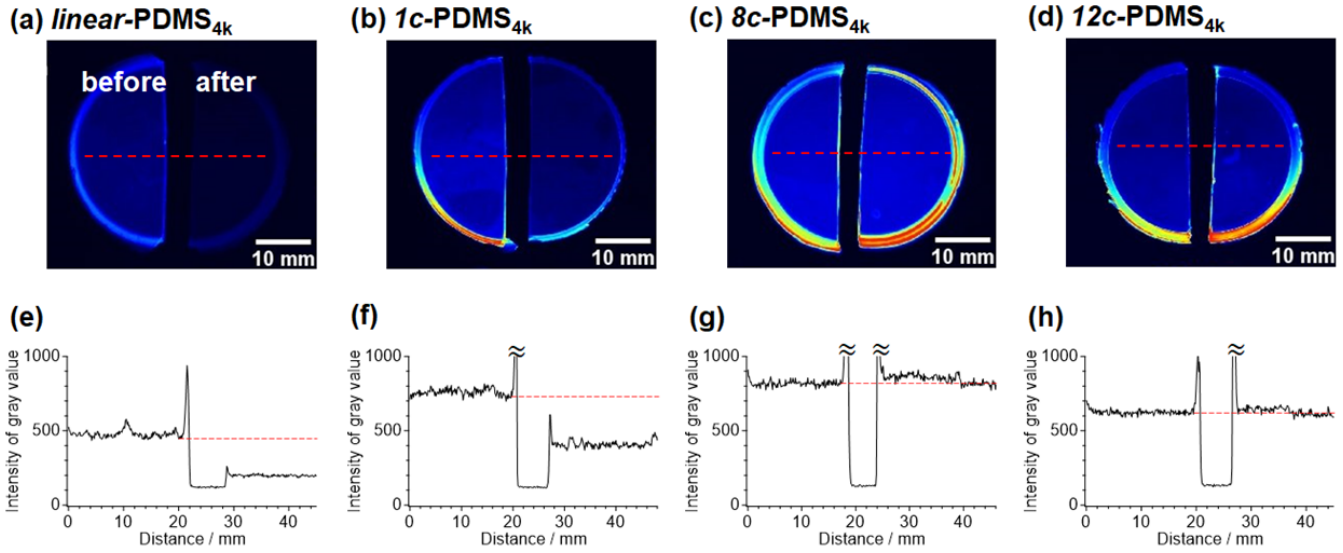


**Figure 5.** Photographs under UV irradiation ($\lambda$ = 302 nm) of the silicone networks prepared in the presence of pyrene-labeled (a) *linear*-PDMS$_{4k}$, (b) *1c*-PDMS$_{4k}$, (c) *8c*-PDMS$_{4k}$, and (d) *12c*-PDMS$_{4k}$. The left and right halves represent the silicone networks before and after soaking in toluene for 5 days, respectively. The luminance extracted along the red lines shown in the photographs (a)–(d) are depicted in (e)–(h).

**Table 3.** Trapping efficiencies in silicone networks with different $M_c$.[a]

| Run | Sample | $M_c$ [b] | % Trapped |
|---|---|---|---|
| 1 | *1c*-PDMS$_{4k}$ | $1.3 \times 10^4$ | 27 ± 12 [c] |
| 2 | | $8.0 \times 10^4$ | 29 |
| 3 | | $0.2 \times 10^4$ | 87 |
| 4 | *16c*-PDMS$_{4k}$ | $1.3 \times 10^4$ | 84 |
| 5 | | $8.0 \times 10^4$ | 81 |
| 6 | *6c*-PDMS$_{26k}$ | $1.3 \times 10^4$ | 100 |
| 7 | | $6.4 \times 10^4$ | 100 |

[a] Each network was prepared in the presence of 10 wt% *mc*-PDMS. [b] Determined by SEC-MALS in $CHCl_3$. [c] Average value for at least two experiments.

To evaluate the effects of ring size on rotaxane formation, we prepared a series of PDMS networks from HO–PDMS$_{13k}$–OH in the presence of 10 wt% *mc*-PDMSs with larger $M_{n,ring}$ ($M_{n,NMR}$ = 14,200 and 25,500). When comparing *1c*-PDMS, the trapping efficiency increased from 27 ± 12% to 75% by increasing the ring size from 4k to 28k (Table 2). This tendency was confirmed both experimentally and computationally. Still, quantitative trapping cannot be achieved using monocyclic PDMS, even at ring sizes larger than $M_e$. In contrast, *4c*-PDMS$_{14k}$ exhibited a higher trapping efficiency (92%), and *11c*-PDMS$_{14k}$ was quantitatively trapped in the network. *6c*-PDMS$_{26k}$ and *10c*-PDMS$_{26k}$ also led to quantitative trapping efficiencies. Fewer rings are required for perfect trapping in the network with large ring sizes (Figure 6).

To exclude the possibility of non-rotaxane trapping, such as slow diffusion in the network due to the high-molecular-weight character of *mc*-PDMS, we attempted further washing of the network containing *6c*-PDMS$_{26k}$ with boiling toluene using a Soxhlet extractor. No *6c*-PDMS$_{26k}$ elution was observed, even after 24 h. We also attempted the topological trapping of *6c*-PDMS$_{26k}$ in a network with a larger 64k $M_c$ (obtained from HO–PDMS$_{64k}$–OH). Given that trapping is based on the slow diffusion in the network, an increase in $M_c$ should reduce the apparent trapping efficiency.[48] However, 100% trapping was observed in this network (Table 3). These results provide solid evidence for the quantitative trapping of rotaxanes in PDMS networks. Considering the large difference in trapping efficiency around $M_e$ (40% for *1c*-PDMS$_{14k}$ and 75% for *1c*-PDMS$_{28k}$), a ring size larger than $M_e$ is vital for achieving high trapping efficiency regardless of the number of cyclic units.

**Figure 6.** Correlation of trapping efficiency, number of cyclic units, and ring size for each *mc*-PDMS in HO–PDMS$_{13k}$–OH silicone networks.

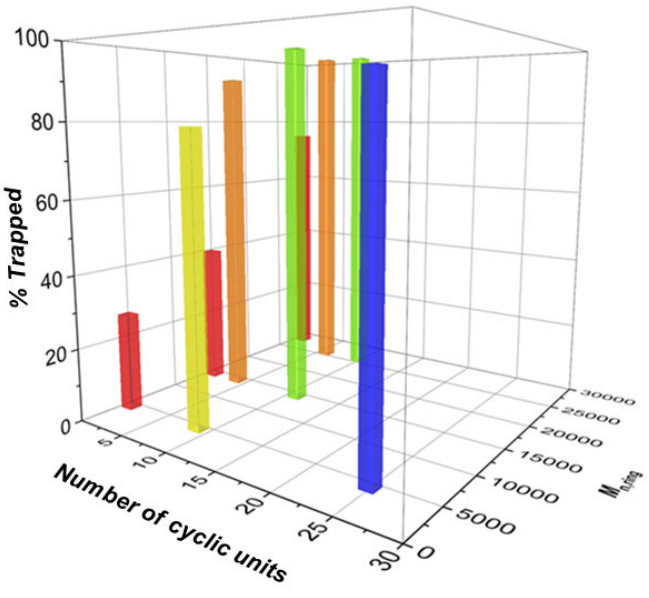

Given these results, we wanted to determine the quantity of *mc*-PDMS that can be topologically trapped in the PDMS network. Thus, we prepared a silicone network by cross-linking HO–$PDMS_{13k}$–OH in the presence of 40 and 60 wt% *6c*-$PDMS_{26k}$. Notably, both silicone networks retained a transparency similar to that prepared with 10 wt% *6c*-$PDMS_{26k}$. Still, they were softer than the network of the 10 wt% blend, likely owing to the reduction in cross-link density upon dilution by trapped *6c*-$PDMS_{26k}$. For the 40 wt% blend, *6c*-$PDMS_{26k}$ elution was not observed upon soaking in toluene, confirming quantitative trapping. For the 60 wt% blend, a significant amount of the soluble fraction was obtained by soaking in toluene, making separately quantifying the sol fraction and non-trapped *6c*-$PDMS_{26k}$ difficult. Nevertheless, the trapping efficiency was estimated to be at least 88%, considering that all soluble fractions were *6c*-$PDMS_{26k}$ (Table 2). Thus, up to 50 wt% of *mc*-PDMS can be topologically trapped quantitatively.

The damping performance of a multicyclic PDMS-blended silicone network was evaluated to demonstrate the potential of topological trapping for industrial applications. Damping materials require a constant high loss factor (tan $\delta$) over a wide range of temperatures and frequencies. Recently, polymer fluid gels, in which a polymer network is filled with a linear polymer fluid, have been proposed as facile and versatile high-performance damping materials.[49] However, the linear polymer fluid could leach over time. Thus, replacing the linear polymer fluid with topologically trapped multicyclic polymer chains can produce a non-leaching polymer fluid gel. To test this hypothesis, rheological measurements were performed on silicone networks prepared in the presence of 60 wt% linear PDMS (*linear*-$PDMS_{41k}$), monocyclic PDMS (*1c*-$PDMS_{37k}$), and multicyclic PDMS (*5c*-$PDMS_{43k}$), and master curves of the modulus vs. frequency created using the time-temperature superposition principle (Figure S3). Figure 7 shows the frequency dependence of tan $\delta$, which is the most crucial characteristic for evaluating damping performance. The tan $\delta$ value for the *linear*-$PDMS_{41k}$-blended sample was higher than that of the bare PDMS network without additional linear or cyclic/multicyclic PDMS. This behavior is consistent with that of a reported polymer fluid gel made of poly(*n*-butyl acrylate), indicating that our PDMS network attained damping performance via the incorporation of linear PDMS. Thus, energy dissipation occurred because of the chain motion of the added *linear*-$PDMS_{41k}$ in the PDMS network upon mechanical stimulation. The *1c*-$PDMS_{37k}$- and *5c*-$PDMS_{43k}$-blended samples also showed higher tan $\delta$ values than the bare PDMS network. Specifically, the tan $\delta$ values at $\omega$ = 1 rad $s^{-1}$ for *linear*-$PDMS_{41k}$-, *1c*-$PDMS_{37k}$-, and *5c*-$PDMS_{43k}$-blended samples were 4.0, 2.4, and 3.6 times higher than those of the bare PDMS network, respectively. Notably, *linear*-$PDMS_{41k}$- and *5c*-$PDMS_{43k}$-blended samples showed similar tan $\delta$ values, validating our hypothesis. A comparable loss factor was observed for the *5c*-$PDMS_{43k}$- and *linear*-$PDMS_{41k}$-blended samples, indicating the same degree of energy dissipation. The fact that such a trend was observed despite the *mc*-PDMS chains being trapped in the form of rotaxanes may reflect the high degree of structural freedom of the macro-rotaxanes. These results demonstrate the potential of multicyclic polymers as non-leaching additives in network polymers.

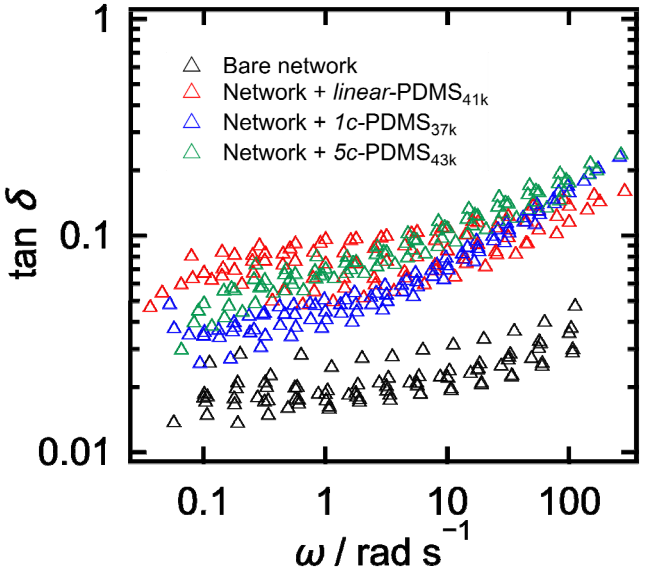


**Figure 7.** Master curves of the loss factor (tan $\delta$) for PDMS networks prepared in the presence of 60 wt% (red) *linear*-$PDMS_{41k}$, (blue) *1c*-$PDMS_{37k}$, and (green) *5c*-$PDMS_{43k}$. The loss factor of the bare PDMS network is also shown (black) for comparison. The reference temperature is 25 °C.

## Conclusions

We have successfully extended the concept of topological trapping to multicyclic polymers using PDMS as a model system. A series of *mc*-PDMSs with a varied number of cyclic units and ring sizes were readily prepared by cyclopolymerization of the corresponding *α,ω*-norbornenyl-functionalized macromonomers. Topological trapping of the synthesized *mc*-PDMS was achieved by *in situ* cross-linking of linear silanol-terminated PDMS using a tetrafunctional cross-linker. The trapping efficiency of *mc*-PDMS was generally high (typically > 80 %), much higher than that of *1c*-PDMS. Notably, a high trapping efficiency was observed when using *mc*-PDMS despite having a ring size much smaller than the entanglement molecular weight ($M_e$) of PDMS. This trend was visually confirmed using pyrene-labeled *mc*-PDMS. Importantly, quantitative topological trapping in the PDMS network was achieved using *mc*-PDMSs with larger $M_{n,ring}$, which is unachievable by the monocyclic polymer. Up to 50 wt% *mc*-PDMS was successfully topologically trapped in the network. These results demonstrate the advantages of using multicyclic polymers to create a novel family of network polymers with additional cross-links via macro-rotaxanes. We are currently investigating the effects of macro-rotaxane formation on the mechanical properties of the PDMS network, which will be reported in the future. Finally, we evaluated the damping performance of a 60 wt% *mc*-PDMS-blended silicone network to demonstrate the potential of topological trapping for industrial applications. Evaluation of the frequency dependence of the tan $\delta$ in *mc*-PDMS-blended samples showed that they had higher damping performance than the bare PDMS network due to energy dissipation through chain motion of the trapped *mc*-PDMS. Considering the quantitative and permanent trapping and high degree of structural freedom of macro-rotaxanes, multicyclic polymers will have a broad range of

applications as non-leaching additives for network polymers. Our systematic evaluation has showcased the many advantages of using multicyclic polymers in topological trapping, providing a foundation for the synthesis and functional applications of macro-rotaxanes.

## Acknowledgements

The authors thank Prof. T. Kawakatsu (Tohoku University), Dr. N. Mashita, Dr. T. Ohkuma, Dr. K. Tsunoda (Bridgestone Corporation), Assistant Prof. F. Li, and Dr. Y. Mato (Hokkaido University) for helpful discussions.

This work was financially supported by a MEXT Grant-in-Aid for Challenging Exploratory Research (19K22209), Grant-in-Aid for Scientific Research (A) (19H00905 and 22H00329), JST CREST (JPMJCR19T4), Photo-excitonic Project (Hokkaido University), Creative Research Institution (CRIS, Hokkaido University), Project of Junior Scientist Promotion at Hokkaido University, and the Eno Scientific Foundation.

**Keywords:** Macro-Rotaxane • Topological Trapping • Silicone Networks • Damping Performance • Cyclic Polymers

## References

[1] J. F. Stoddart, *Angew. Chem. Int. Ed.* **2017**, *56*, 11094–11125.
[2] W. Yang, Y. Li, H. Liu, L. Chi, Y. Li, *Small* **2012**, *8*, 504–516.
[3] R. A. van Delden, M. K. J. ter Wiel, M. M. Pollard, J. Vicario, N. Koumura, B. L. Feringa, *Nature* **2005**, *437*, 1337–1340.
[4] J. Zhao, Z. Zhang, L. Cheng, R. Bai, D. Zhao, Y. Wang, W. Yu, X. Yan, *J. Am. Chem. Soc.* **2022**, *144*, 872–882.
[5] A. Harada, Y. Takashima and H. Yamaguchi, *Chem. Soc. Rev.* **2009**, *38*, 875–882.
[6] L. Chen, X. Sheng, G. Li, F. Huang, *Chem. Soc. Rev.* **2022,** *51*, 7046–7065.
[7] Y. Okumura, K. Ito, *Adv. Mater.* **2001**, *13*, 485–487.
[8] C. Liu, N. Morimoto, L. Jiang, S. Kawahara, T. Noritomi, H. Yokoyama, K. Mayumi, K. Ito, *Science* **2021**, *372*, 1078–1081.
[9] K. Kato, M. Taniguchi, K. Ito, *Macromolecules* **2023**, *56*, 1810–1817.
[10] H. Gotoh, C. Liu, A. B. Imran, M. Hara, T. Seki, K. Mayumi, K. Ito, Y. Takeoka, *Sci. Adv.* **2018**, *4*, eaat7629.
[11] R. A. Pérez, J. v. López, J. N. Hoskins, B. Zhang, S. M. Grayson, M. T. Casas, J. Puiggalí, A. J. Müller, *Macromolecules* **2014**, *47*, 3553–3566.
[12] J. V. López, R. A. Pérez-Camargo, B. Zhang, S. M. Grayson, A. J. Müller, *RSC Adv.* **2016**, *6*, 48049–48063.
[13] R. Watanabe, M. Noba, T. Uno, T. Itoh, M. Kubo, *J. Polym. Sci.* **2020**, *58*, 1982–1988.
[14] M. B. Ruiz, R. A. Pérez-Camargo, J. V. López, E. Penott-Chang, A. Múgica, O. Coulembier, A. J. Müller, *Int. J. Biol. Macromol.* **2021**, *186*, 255–267.
[15] T. Iwamoto, Y. Doi, K. Kinoshita, A. Takano, Y. Takahashi, E. Kim, T.-H. Kim, S. Takata, M. Nagao, Y. Matsushita, *Macromolecules* **2018**, *51*, 6836–6847.
[16] T. Iwamoto, Y. Doi, K. Kinoshita, Y. Ohta, A. Takano, Y. Takahashi, M. Nagao, Y. Matsushita, *Macromolecules* **2018**, *51*, 1539–1548.
[17] M. Kapnistos, M. Lang, D. Vlassopoulos, W. Pyckhout-Hintzen, D. Richter, D. Cho, T. Chang, M. Rubinstein, *Nat. Mater.* **2008**, *7*, 997–1002.
[18] D. Parisi, J. Ahn, T. Chang, D. Vlassopoulos, M. Rubinstein, *Macromolecules* **2020**, *53*, 1685–1693.
[19] K. Hagita, T. Murashima, *Macromolecules* **2021**, *54*, 8043–8051.
[20] J. Mo, J. Wang, Z. Wang, Y. Lu, L. An, *Macromolecules* **2022**, *55*, 1505–1514.
[21] W. Wang, C. S. Biswas, C. Huang, H. Zhang, C.-Y. Liu, F. J. Stadler, B. Du, Z.-C. Yan, *Macromolecules* **2020**, *53*, 658–668.
[22] K. Hagita, T. Murashima, *Polymer* **2021**, *218*, 123493.
[23] G. S. Grest, T. Ge, S. J. Plimpton, M. Rubinstein, T. C. O'Connor, *ACS Polymers Au* **2023**, *3*, 209–216.
[24] L. Garrido, J. E. Mark, S. J. Clarson, J. A. Semlyen, *Polym. Commun.* **1985**, *26*, 53–55.
[25] S. J. Clarson, J. E. Mark, J. A. Semlyen, *Polym. Commun.* **1986**, *27*, 244–245.
[26] L. C. DeBolt, J. E. Mark, *Macromolecules* **1987**, *20*, 2369–2374.
[27] R. Bischoff, S. E. Cray, *Prog. Polym. Sci.* **1999**, *24*, 185–219.
[28] B. R. Wood, S. J. Joyce, G. Scrivens, J. A. Semlyen, P. Hodge, R. O'Dell, *Polymer* **1993**, *34*, 3059–3063.
[29] W. Huang, H. L. Frisch, Y. Hua, J. A. Semlyen, *J. Polym. Sci. A Polym. Chem.* **1990**, *28*, 1807–1812.
[30] T. J. Fyvie, H. L. Frisch, J. A. Semlyen, S. J. Clarson, J. E. Mark, *J. Polym. Sci. A Polym. Chem.* **1987**, *25*, 2503–2509.
[31] T. S. Stukenbroeker, D. Solis-Ibarra, R. M. Waymouth, *Macromolecules* **2014**, *47*, 8224–8230.
[32] K. Hagita, T. Murashima, M. Ebe, T. Isono, T. Satoh, *Polymer* **2022**, *245*, 124683.
[33] K. Hagita, T. Murashima, *Polymer* **2021**, *223*, 123705.
[34] T. Isono, T. Sasamori, K. Honda, Y. Mato, T. Yamamoto, K. Tajima, T. Satoh, *Macromolecules* **2018**, *51*, 3855–3864.
[35] Y. Mato, M. Sudo, H. Marubayashi, B. J. Ree, K. Tajima, T. Yamamoto, H. Jinnai, T. Isono, T. Satoh, *Macromolecules* **2021**, *54*, 9079–9090.
[36] H. Oike, M. Hamada, S. Eguchi, Y. Danda, Y. Tezuka, *Macromolecules* **2001**, *34*, 2776–2782.
[37] K. Urayama, T. Kawamura, S. Kohjiya, *Polymer* **2009**, *2*, 347–356.
[38] M. Lejars, A. Margaillan, C. Bressy, *Chem. Rev.* **2012**, *112*, 4347–4390.
[39] C. Chen, J. Wang, Z. Chen, *Langmuir* **2004**, *20*, 10186–10193.
[40] B. P. Mayer, J. P. Lewicki, T. H. Weisgraber, W. Small, S. C. Chinn, R. S. Maxwell, *Macromolecules* **2011**, *44*, 8106–8115.
[41] J. E. Mark, R. R. Rahalkar, J. L. Sullivan, *J. Chem. Phys.* **1979**, *70*, 1794–1797.
[42] J. E. Mark, M. A. Llorente, *J. Am. Chem. Soc.* **1980**, *102*, 632–636.
[43] S. M. Aharoni, *Macromolecules* **1986**, *19*, 426–434.
[44] Y. H. Zang, P. J. Carreau, *J. Appl. Polym. Sci.* **1991**, *42*, 1965–1968.
[45] M. Appel, G. Fleischer, *Macromolecules* **1993**, *26*, 5520–5525.
[46] L. J. Fetters, D. J. Lohse, D. Richter, T. A. Witten, A. Zirkel, *Macromolecules* **1994**, *27*, 4639–4647.
[47] K. Urayama, T. Kawamura, S. Kohjiya, *Polymer* **2009**, *50*, 347–356.
[48] K. Urayama, K. Yokoyama, S. Kohjiya, *Macromolecules* **2001**, *34*, 4513–4518.
[49] J. Huang, Y. Xu, S. Qi, J. Zhou, W. Shi, T. Zhao, M. Liu, *Nat. Commun.* **2021**, *12*, 3610.

## Entry for the Table of Contents

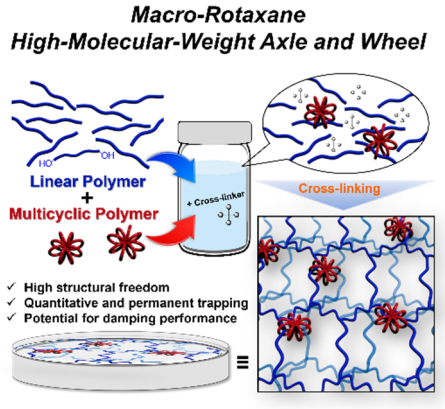


"Macro-rotaxanes" which consist of high-molecular-weight axle and wheel components were constructed by *in situ* cross-linking of linear polymers in the presence of multicyclic polymers. The concept of topological trapping was extended to multicyclic polymers and it was found that multicyclic polymers with more cyclic units and larger ring sizes can be quantitatively trapped. Up to 50 wt% were successfully topologically trapped as macro-rotaxanes.